Performance Analysis of IEEE 802.15.6-Based Coexisting Mobile WBANs With Prioritized Traffic and Dynamic Interference

Xiaoming Yuan, *Student Member, IEEE*, Changle Li, *Senior Member, IEEE*, Qiang Ye, *Member, IEEE*,
Kuan Zhang, *Member, IEEE*, Nan Cheng, *Member, IEEE*, Ning Zhang, *Member, IEEE*,
and Xuemin Shen, *Fellow, IEEE*

Abstract—Intelligent wireless body area networks (WBANs) have entered into an incredible explosive popularization stage. WBAN technologies facilitate real-time and reliable health monitoring in e-healthcare and creative applications in other fields. However, due to the limited space and medical resources, deeply deployed WBANs are suffering severe interference problems. The interference affects the reliability and timeliness of data transmissions, and the impacts of interference become more serious in mobile WBANs because of the uncertainty of human movement. In this paper, we analyze the dynamic interference taking human mobility into consideration. The dynamic interference is investigated in different situations for WBANs coexistence. To guarantee the performance of different traffic types, a health critical index is proposed to ensure the transmission privilege of emergency data for intra- and inter-WBANs. Furthermore, the performance of the target WBAN, i.e., normalized throughput and average access delay, under different interference intensity are evaluated using a developed three-dimensional Markov chain model. Extensive numerical results show that the interference generated by mobile neighbor WBANs results in 70% throughput decrease for general medical data and doubles the packet delay experienced by the target WBAN for emergency data compared with single WBAN. The evaluation results greatly benefit the network design and management as well as the interference mitigation protocols design.

Index Terms—Wireless body area network (WBAN), interference, CSMA/CA, IEEE 802.15.6, Markov chain model.

I. INTRODUCTION

WIRELESS Body Area Networks (WBANs) are human-centered, highly reliable short range wireless communication networks [1]. With flexibility, scalability and low-cost characteristics, WBANs have been widely used to provide real-time and continuous care for health monitoring in e-healthcare [2]. The application of WBAN alleviates the conflicts between limited healthcare resources and increasing needs of aging population. WBAN technology has been envisioned as one of the primary technologies for the ubiquitous Internet-of-Things (IoT) to enhance the quality of people's life [3]–[5].

WBANs are widely deployed in densely populated scenarios, for example, wards and waiting rooms in hospitals, resident-centered nursing homes, and even public transports. The communication zones of adjacent WBANs are close or even overlapped. Coexisting densely deployed WBANs inevitably suffer severe intra- and inter- WBAN interference. Intra-WBAN interference occurs when nodes in a WBAN transmit data at the same time. Inter-WBAN interference is caused by simultaneous data transmission among two or more adjacent WBANs. Inter-WBAN interference decreases the reliability and timeliness of physiological data transmission, increasing the network management and economic cost paid on healthcare. Particularly, interference may lead to catastrophic incomplete or overdue data in emergency medical diagnosis and threaten the life safety of people. Therefore, interference problem of coexisting multi-WBANs needs in-depth study.

Many researchers have paid attention to the interference of coexisting WBANs. The inter-user interference among adjacent WBANs is investigated in [6]. An interference distribution model [7] is proposed by using a geometrical probability approach. The inter-WBAN interference is related to the activities of users carrying them and is different from other types of wireless networks [8]. The traditional interference mitigation approaches are not suitable for WBANs. The inter-WBAN

X. Yuan and C. Li are with the State Key Laboratory of Integrated Services Networks, Xidian University, Xi'an 710071, China (e-mail: xmyuan@stu.xidian.edu.cn; clli@mail.xidian.edu.cn).

Q. Ye, N. Cheng, and X. Shen are with the Department of Electrical and Computer Engineering, University of Waterloo, Waterloo, ON N2L 3G1, Canada (e-mail: q6ye@uwaterloo.ca; n5cheng@uwaterloo.ca; sshen@uwaterloo.ca).

K. Zhang is with the Department of Electrical and Computer Engineering, University of Nebraska-Lincoln, Omaha, NE 68182 USA (e-mail: kuan.zhang@unl.edu).

N. Zhang is with the Department of Computing Sciences, Texas A&M University–Corpus Christi, Corpus Christi, TX 78412 USA (e-mail: ning.zhang@tamucc.edu).

Color versions of one or more of the figures in this paper are available online at http://ieeexplore.ieee.org.

Digital Object Identifier 10.1109/TWC.2018.2848223

coexistence and interference mitigation schemes are surveyed and discussed in [9]. A Bayesian game based power control scheme [10] is introduced to mitigate the impact of inter-WBAN interference. A beacon interval shifting scheme [11] and a beacon scheduling scheme [12] are developed to execute carrier sensing before beacon transmission to reduce inter-WBAN interference.

However, in the study of interference analysis and interference mitigation, there are few work considering the dynamic interference of mobile neighbor WBANs. Mobility of WBANs affects the service-oriented as well as the application-oriented network performance [13]. Interference intensity varies with human movements. Interference lasts for a short period when neighbor WBAN just passes by or lasts long when there is no relative movement between inter-WBANs. Network performance, i.e., throughput and delay, fluctuate with interference variation and become severe when adjacent WBANs are deeply overlapped with each other [14]. Therefore, analyzing the dynamic interference in coexisting multi-WBANs is required, which satisfies the practical scenario well and can greatly benefit network design and management.

On the other hand, different types of traffic in the WBAN have different Quality-of-Service (QoS) requirements. For example, life-critical emergency electroencephalogram (EEG) and electrocardiogram (ECG) data require high reliability and low transmission delay while regular temperature data are delay-tolerant. It is necessary to differentiate the traffic priorities to satisfy the diversified performance requirements. In addition, some monitoring physiological data in medical services exceed the normal range and trigger other abnormal changes occasionally. The variation message and the abnormal data have higher priority than usual, and they should be transmitted to the hub or data center timely for further processing. Both of the general data and the abnormal data are required to be considered in multi-WBANs coexistence.

In this paper, we analyze the interference of coexisting WBANs by considering human mobility and traffic differentiation. The network topology changes when human moves. Different nodes with different traffic priorities in the network have diverse performance requirements. In this case, the asynchronous IEEE 802.15.6-based Carrier Sense Multiple Access with Collision Avoidance (CSMA/CA) protocol [15] is employed rather than the scheduled Time Division Multiple Address (TDMA). The CSMA/CA scheme is adaptive to the network topology and network load changes, and it does not require complex time synchronization compared to TDMA method. We develop the CSMA/CA Medium Access Control (MAC) mechanism in this paper to improve the flexibility and scalability of a WBAN. We investigate the MAC performance with interference dynamics from neighboring WBANs and guarantee the required QoS for different types of traffic. Our main contributions is summarized as follows.

- Firstly, we analyze dynamic inter-WBAN interference with the movement of neighbor WBANs in rectilinear motion and curvilinear motion cases. We also investigate the interference dynamics in different situations for a multi-WBANs coexistence scenario (e.g. different distances between inter-WBANs, varying number of nodes

of each WBAN, different number of coexisting WBANs, etc.). Furthermore, we consider the interference dynamics in developing the performance analytical model, which facilitates the practicability and credibility of the model in WBANs.

- Secondly, we propose a health critical index to guarantee the privilege of time sensitive emergency and burst medical data traffic. The definition of the health critical index takes into account service types, traffic differentiation, and data severity. The burst abnormal data enjoy higher health critical index value to ensure the channel access privilege than other normal data. In addition, an algorithm is designed to manage the service order of all the nodes in multi-WBANs coexistence scenario.

- Finally, we develop a three-dimensional Markov chain performance analytical model to investigate the impact of interference on throughput and packet access delay of prioritized traffic in the target WBAN. Extensive numerical results demonstrate the accuracy and effectiveness of our proposed performance analytical framework.

The remainder of paper is organized as follows. Section II summarizes the related work. The network model and traffic model is presented in Section III. In Section IV, the changing interference and the proposed severity index are described. Performance on normalized throughput and average packet access delay are analyzed in Section V. Section VI demonstrates analytical results and discussions. Finally, concluding remarks and future work outlines are given in Section VII.

II. RELATED WORK

Multiple WBANs coexist in one place in order to access to healthcare services for different patients. The interference from neighbor WBANs is inevitable in dense area, degrading network performance and increasing network management cost [16]. Interference in multiple WBANs include the mutual or inter-user interference incurred by simultaneous transmissions in the vicinity of multiple WBANs, and cross-technology interference caused by the utilization of different transmission technologies operating in the same spectrum range [17]. More and more researchers have paid their attention on interference analysis and mitigation in coexisting WBANs.

The coexistence and interference management issues were summarized [18], exploring a wide variety of communication standards and methods deployed in WBAN. Sun *et al.* [19] presented a stochastic geometry analysis model to analyze the inter-user interference in IEEE 802.15.6 based WBANs and derived the optimal interference detection range to tradeoff between outage probability and spatial throughput. Jameel *et al.* [20] analyzed the impact of co-channel interference on WBANs under generalized fading. The progress of interference generation between two deeply overlapped WBANs [21] was introduced. Three heuristic solutions [22] were presented to solve the problems of mutual interference and cross-technology interference. The nodes of intra-WBAN employed the IEEE 802.15.4 protocol [23] with not distinguishing the traffic priorities. Zhang *et al.* [24] described the

TABLE I
BASIC NOTATIONS

Parameter	Description	Parameter	Description
Υ	Interference range of hub	H_m^y	Health critical index value of node y in N_m
N_m	WBAN m	P_{idle}	Probability of the channel being idle
d_m	The distance between N_m and target WBAN	R_s	Symbol rate
UP_k	User (or traffic) priority for a node	P_b	Probability of packet collision
l	Failure times before the successful transmission	P_u	Probability of backoff counter being unlocked
τ_k	Medium access probability of UP_k node	T_{c-slot}	CSMA slot length
Y	The number of nodes in a WBAN	T_{pk}	Packet transmission time
n_k	The number of nodes of UP_k	N_{total}	Total bits flowing in the physical layer
n_I	The number of interfering nodes	BT_{max}	The maximum backoff stage
$CW_{\min[UP_k]}$	Minimum contention window (CW) value of UP_k	$W_{k,j}$	CW value of UP_k at jth backoff stage
$CW_{\max[UP_k]}$	Maximum CW value of UP_k	T_{kCW}	Mean backoff time
$P_{UP_k-inlock}$	Probability that the backoff counter is locked due to insufficient remaining time for a transaction	P_{kidle}	Probability of channel being idle during the backoff period of UP_k node

necessity of classifying different types of health data for a WBAN.

Moreover, different analytical models and proposed algorithms are used in the MAC performance analysis for WBANs. In the presence of inter-user interference, a stochastic geometry model [25] were proposed to analyze the effects of IEEE 802.15.6 MAC. The outage probability and spatial throughput of WBANs were derived on the spatial distribution of the interfering WBANs. An analytical model for the IEEE 802.15.4 MAC protocol [26] was proposed to explore the time-varying feature of the MAC statistics under periodic traffic. Based on Bianchi's work [27], many authors contributed to the Markov analytical models for WBANs [28]–[31]. A criticality index was introduced [28] to identify the critical physiological parameter, using a Markov chain-based analytical approach to maximize the reliability of the critical node. Nevertheless, the different User Priorities (UPs) of various traffic in a WBAN should be considered. A four dimensional Markov chain [30] was used to evaluate the power consumption, throughput and average delay concerned the time spent by a node awaiting the acknowledgement frame. The IEEE 802.15.6 CSMA/CA mechanism with different UPs was analyzed employing a three-dimensional Markov chain model [31]. The proposed scheduling techniques [32] were evaluated within various traffic rates and time slot lengths to improve WBAN reliability and energy efficiency. However, these works are more comprehensive if they considered the traffic critical conditions out of safety range and the influence of interference from adjacent WBANs.

Several approaches were proposed to mitigate the intra- and inter- WBAN interference [33]–[39]. A superframe overlapping scheduling method [33] based on beacon shifting and superframe interleaving interference mitigation techniques was developed for coexisting WBANs. A two-layer interference mitigation MAC protocol (2L-MAC) was proposed based on IEEE 802.15.6 for WBANs [34]. However, the scheme evaluated the long-term interference in non-adaptive and scheduled one node for transmission regardless of the interference level. Cheng and Huang [36] employed TDMA method to reduce mutual interference of nearby WBANs. A horse racing scheduling scheme [37] was raised to decrease single-WBAN interference. But the resource allocation scheme might degrade

once the topology of a WBAN changes with human movements. Therefore, the random adaptive CSMA/CA method is more suitable in the analysis of interference dynamics with human movements and diversity traffic types. The authors [39] proposed an adaptive CSMA/CA MAC protocol by adjusting the length of each polling period/MAC frame based on its perceived interference level to mitigate the inter-WBAN interference.

III. SYSTEM MODEL

In this section, we present the network model as well as the traffic model. Some important notations used in the paper are summarized in Table I.

A. Network Model

The WBAN usually consists of a centralized entity hub and a number of sensor nodes to monitor the vital signs of human body. The Hub is usually performed by a smartphone or a Personal Digital Assistant (PDA), which has greater computing capability with power-rechargeable. Sensor nodes collect EEG, ECG, motion signals, and general physiological data. There is a set of coexisting WBANs $\{N_m | m = 1, 2, \ldots, M\}$ in the system, as shown as in Fig. 1, where M is the number of WBANs and N_m stands for WBAN m. The hub is denoted by $\{N_{mh} | m = 1, 2, \ldots, M\}$ and several numbered physiological sensor nodes are denoted by $\{s_m^y | y = 1, 2, \ldots, Y\}$.

There are four communications types in WBANs, namely in-body, on-body, off-body and body-to-body [40]. Usually, the collected data traffic is transmitted from nodes to hub through on-body channel and from hub to the data center through free space wireless channel. The body-to-body type represents communications from one person's body to another person's body. In general, the distance between WBANs is large enough such that there is no inter-WBAN interference, just as the non-intrusive distribution of N_3 and N_4. With the movement of human body, the distance between WBANs is constantly changing. As the inter-WBANs distance decreases, the communication zones are overlapped partially. The interference occurs between the adjacent WBANs if there are senor nodes in the communication area of neighbor WBANs, as the distribution of N_1, N_2 and N_3 in Fig. 1. The data transmissions
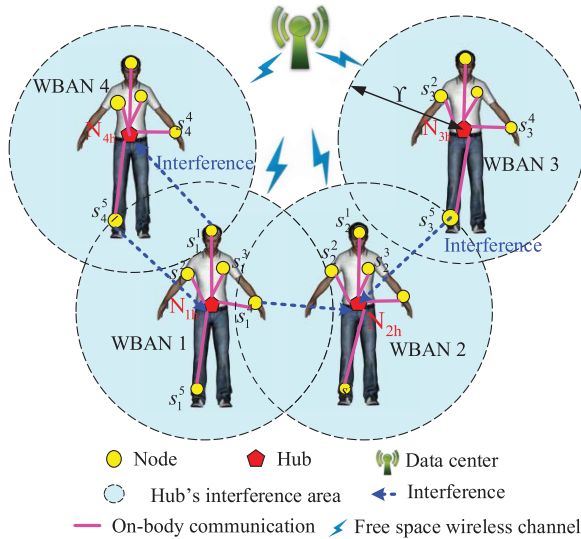
Fig. 1. Network model.

TABLE II

UP MAPPING AND CW BOUNDS

User priorities	Traffic designation	CWmin	CWmax
7	Emergency or medical implanted event report	1	4
6	High priority medical data or network control	2	8
5	Medical data or network control	4	8
4	Voice data or management	4	16
3	Video data	8	16
2	Excellent effort data	8	32
1	Best effort data	16	32
0	Background data	16	64

of sensor node s_1^4 in the overlapped area of N_1 and N_2 intrude all the data transactions of N_2, since s_1^4 is in the interference range of hub N_{2h}. s_3^5 in N_3 also interferes data transactions in N_2, increasing the data collision probability. If the inter-WBAN distance becomes smaller, the overlapped area as well as the number of interference nodes increases. The worst case is that two or more communication zones are completely overlapping. The interference seriously aggravates the network performance.

B. Traffic Model

Sensor nodes in each WBAN collect and transmit realtime sensing data to the hub. Different sensing data types have different reliability and delay requirements, especially the life-critical emergency data in medical applications which require high reliability and minimum transmission delay. The sensing health data are classified into different data or user priorities to satisfy the diversified performance requirements. In IEEE 802.15.6, eight User Priorities (UPs) are predefined in Table II. The higher user priority has privilege to access the channel. The user priorities of medical data traffic are from 5 to 7, guaranteeing the severer traffic in high priority to be transmitted timely. We consider each node in the WBAN only collects one kind of user priority traffic and the WBAN is

TABLE III

WBAN PRIORITY OF SERVICE

BAN priorities	WBAN services
3	Highest priority medical services
2	General health services
1	Mixed medical and non-medical services
0	Non-medical services

saturated that every node in the network always has packets to contend to access the channel. Data with higher user priority enjoy small Contention Window (CW) size to guarantee the low access delay.
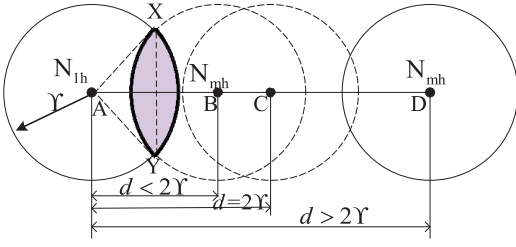
The definition of user priority is based on the collected data. The collected data are used to provide various applications and services (medical or non-medical services). The definition of BAN priority is from the perspective of applications. In multi-WBANs coexistence scenario, it is necessary to classify the BAN priority with different services among inter-WBANs. Different applications may collect the same kind of data. For example, both interactive motion sensing games and medical applications for disability assistance are required to collect the motion data. According to the traffic designation in Table II, the motion data have the same kind of user priorities and contention window. The collision probability increases when the same UP data are transmitted at the same time in neighbor interference area. But the motion data require lower delay and higher reliability for medical service than that for entertainment. Therefore, we differentiate the BAN priority besides the user priority, as shown in Table III. The medical application takes precedence over other non-medical applications. The BAN priority guarantees the privilege of nodes accessing the channel for health monitoring, especially in the condition of existing few interference nodes in multiple WBANs coexistence scenario.

IV. INTERFERENCE OF COEXISTENCE MOBILE WBANS

The mutual interference of multi-WBAN coexistence is caused by the concurrent data transactions of sensor nodes from neighbor WBANs. In other words, the body-to-body communications generate interference. Human, as the wearer of WBAN, is not static. The slow or quick movement leads to channel dynamics. The body-to-body WBAN interference channel modeling with movement can be found in [41] and [42]. In this section, we first calculate the changing interfering nodes and discuss the dynamic interference of multiple coexisting WBANs in different cases. Then we propose a health critical index to guarantee the transmission privilege of emergency data of a particular node or WBAN in multi-WBAN coexistence scenario.

A. Dynamic Interference of Coexisting Mobile WBANs

The human mobility is reflected by the velocity and direction angle of WBAN movement. The interference channel gain is dominated mostly by human movements [43]. For very slow movement, the channel coherence time is relative long, and the interference channel gain could be considered unchanged. The

Fig. 2.   The relative position of N_1 and N_m.

(a) Rectilinear motion

(b) Redirection curvilinear motion

Fig. 3.   The relative motion of N_m.

channel fading and path loss of the movement is negligible. In this paper, we pay our attention to the influence of changing interference intensity related to human mobility on network performance, instead of how human movement manners affect time varying interference channel.

The number of sensor nodes attached on a human body varies depending on the individual requirements. We assume all the WBANs are in same configuration. The topology of a WBAN can be modeled as a hub centered circle. The hub is located near the center of a human body with the communication range Υ. We consider that the interference range of sensor nodes is the same as communication range Υ. The projections of all the nodes are relative uniformly random distribution within the circle. The modeled topology of a WBAN is two dimensional for the tractable analysis instead of the three-dimensional distribution in reality.

Assuming N_1 as the target WBAN, we firstly pay our attention to the impact of one existing neighbour WBAN N_m. Every hub knows its coordinate in the network. The coordinates of N_{1h} and N_{mh} are (x_1, y_1) and (x_m, y_m), respectively. The inter-WBAN distance d between N_1 and N_m is defined as the distance from N_{1h} to N_{mh}. The distance d can be calculated as

$$d = \sqrt{(x_m - x_1)^2 + (y_m - y_1)^2} \qquad (1)$$

WBAN movements lead to changing relative distance of inter-WBANs. If an arbitrary WBAN N_m moves in the direction of target WBAN N_1, there are three relative positions of the two WBANs, as shown in Fig. 2. If $d > 2\Upsilon$, there is no inference between them. N_m keeps moving from position D to position C, then it reaches the edge that can interfere N_1. We mark this critical point $d = 2\Upsilon$ as the moment $t = 0$. Supposing that N_m continues moving to N_1 till position B where d is less than 2Υ resulting in an overlap of the communication zones. Sensor nodes of N_m in the overlapped area become interference sources, increasing the collision probability of data transactions of the target WBAN and degrading the network performance on throughput and packet delay at the same time. The interference duration ends at the moment when the inter-WBAN distance d equals 2Υ the next time.

The moving direction of N_m at next moment is uncertain since people have a variety of options. In this paper, the movement of N_m could be classified into two cases: rectilinear motion and redirection curvilinear motion. The velocity of N_{mh} is denoted by v_m. The direction angle between the
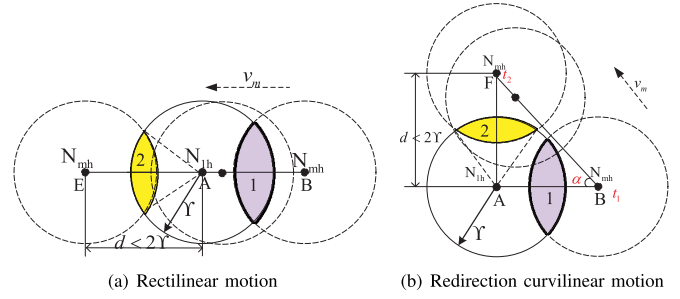
leaving and the approaching direction of N_{mh} is α. The rectilinear motion of N_m means the directional angle α is zero or π, as shown in Fig. 3(a). N_{mh} moves from position B to position E. Section 1 is the original overlapping area while section 2 is the overlapping area at the next moment. The curvilinear motion refers that the value of α ranges in $(0, \pi)$, as shown in Fig. 3(b). N_{mh} moves from position B at moment t_1 to position F at moment t_2. The value of α could be acquired in the law of cosines from Eq. (2).

$$\cos \alpha = \frac{d_{t_1}^2 + d_{m\Delta t}^2 - d_{t_2}^2}{2 d_{t_1} d_{m\Delta t}} \qquad (2)$$

where d_{t_1} and d_{t_2} are the inter-WBAN distance at moment t_1 and t_2, respectively. $d_{m\Delta t}$ is the straight-line distance of N_{mh} in the time duration Δt ($\Delta t = t_2 - t_1$). When N_{mh} is in continuous movements, we can get $d_{m\Delta t} = \sqrt{(x_{mt_2} - x_{mt_1})^2 + (y_{mt_2} - y_{mt_1})^2} = v_m(t_2 - t_1)$. The directional angle α and the value of v_m affect the interference duration.

The interference intensity is directly decided by the number of interference nodes n_I, which is related to the inter-WBAN distance d. The intersection area of the target WBAN N_1 and N_m is twice of the difference between sector area (S_{XAY}) and triangle area ($S_{\triangle XAY}$), as shown in Fig. 2. Therefore, the n_I can be obtained from Eq. (3).

$$n_I = \frac{2Y}{\pi \Upsilon^2} \times \left(\arccos \frac{d}{2\Upsilon} \Upsilon^2 - \frac{d}{2} \sqrt{\Upsilon^2 - \frac{d^2}{4}} \right) \qquad (3)$$

where Y is the number of sensor nodes in a WBAN. The maximum n_I can be reached at $d = 0$ where the two WBANs are totally overlapped, the value of which is Y. The interference nodes continuously affect the performance of N_1 until N_m leaves.

For the coexistence of more than two WBANs, the distance between any WBAN and the target WBAN affects the number of interference nodes. It makes no great difference to the target WBAN whether the other WBANs have overlap or not. In other words, we only focus on the number of nodes in the interference range of target WBAN and ignore the interference among any other WBANs. One case that any two of the three WBANs have an overlap is described in Fig. 4. The number of interference nodes to the target WBAN N_1 equals the sum of interfering nodes from N_p and N_q in the interference range
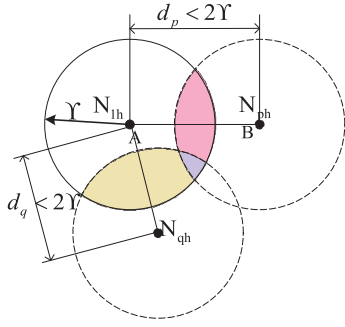
Fig. 4.   The relative position of three WBANs.

and can be obtained using Eq. (4).

$$n_I = \frac{2Y}{\pi} \left(\arccos \frac{d_p}{2\Upsilon} + \arccos \frac{d_q}{2\Upsilon} \right)$$
$$- \frac{Y}{\pi \Upsilon^2} \left(d_p \sqrt{\Upsilon^2 - \frac{d_p^2}{4}} + d_q \sqrt{\Upsilon^2 - \frac{d_q^2}{4}} \right) \quad (4)$$

where $d_p = \sqrt{(x_p - x_1)^2 + (y_p - y_1)^2}$ and $d_q = \sqrt{(x_q - x_1)^2 + (y_q - y_1)^2}$, respectively.

Given that there are M WBANs in the WBAN coexistence scenario, the potential interference sources set to the target WBAN at moment t can be represented as $\{N_K | 0 \leq K \leq M; \forall K, d_k < 2\Upsilon \}$. Calculating the whole intersection area of the target WBAN N_1 and interference WBAN $N_K (0 \leq K \leq M)$, we can get the total number of interference nodes by Eq. (5).

$$n_I = \frac{2Y}{\pi \Upsilon^2} \sum_{m \in K} \left(\arccos \frac{d_m}{2\Upsilon} \Upsilon^2 - \frac{d_m}{2} \sqrt{\Upsilon^2 - \frac{d_m^2}{4}} \right) \quad (5)$$

where d_m is the distance from an arbitrary WBAN m in the interference source sets to the target WBAN. d_m and n_I are affected by the directional angle and the velocity v_m of WBAN m.

B. Health Critical Index

The definition of critical index indicate the ratio of deviation in sensed physiological data and the normal value of that physiological parameter is proposed in [44]. The critical index is used to assist a data-rate tuning mechanism for resource sharing [44]. The mechanism is IEEE 802.15.4-based, without differentiating the traffic priority and the access privilege of the nodes as well as the interference problem. A fuzzy inferencing-based health criticality assessment approach followed by an efficient decision making model based on the concepts of Markov decision process [45] is proposed to optimize the energy consumption in WBAN. It takes body temperature and human age as the influential criteria. However, the work in [45] focuses on the individual instead of the multi-WBANs coexistence. To guarantee the transmission delay of time sensitive emergency and burst data, the heath critical index (H) is introduced to determine the order of nodes enjoying service and transmission in multi-WBAN coexistence with interference.

TABLE IV
PAIRWISE COMPARISON MATRIX

	UPs	SI	BP	Weight factor ρ
UPs	1	1/5	1/5	0.15
SI	5	1	1/3	0.51
BP	5	3	1	0.34

The heath critical index H in our paper considers the traffic user priority, WBAN priority (BP) and the severity condition. The H helps select the critical data among multiple nodes in the WBANs coexistence scenario. Then the node with emergency data performs the CSMA/CA contention progress to access the channel. The traffic priority UP_k and WBAN priority BP_m can be found in Table II and Table III. We use the severity index (SI) denotes the degree of data deviating from the safety range. The details of this severity index are available in the original paper [46]. The value of SI satisfies $0 \leq SI \leq 1$. The values of H can be obtained through Eq. (6).

$$H = \rho_1 \times \frac{UP_k}{7} + \rho_2 \times SI + \rho_3 \times \frac{BP_m}{3}, \quad \rho_1 + \rho_2 + \rho_3 = 1 \quad (6)$$

where ρ_1 is the weight factor of the user priority, ρ_2 is the weight factor of the data critical condition while ρ_3 is corresponding to the BAN priority. The values of the weight factors could be calculated according to the Analytic Hierarchy Process (AHP) method [47], [48].

The AHP method provides an effective solution to quantify qualitative problems through pairwise comparisons. The comparisons are made using a scale of numbers that indicates, how much more, one element dominates another in regard to the criterion or property. The fundamental scale of absolute numbers is from 1 to 9. The minimum value 1 means the two attributes contribute equally to the objective while the maximum value 9 means one attributes is extreme important over another.

Three attributes are considered in the paper, i.e. WBAN priority, user priority, and severity condition. The WBAN priority is strongly important over data deviation. Data severity is more important than user priority. In other words, nodes for medical applications have privilege than non-medical applications. Nodes in abnormal condition have higher heath critical index value than that of normal, which gets preferential order to access to services. For example, the monitoring data of a UP_5 node in a serious fluctuation are more important than a UP_6 node in normal condition. The pairwise comparison matrix of the three attributes with respect to the H is shown in Table IV. The attributes listed on the left are matched one by one to each attribute listed on top according to their importance with respect to the health critical index. The weight factors are obtained by Asymptotic Normalization Coefficient (ANC). The derived weight factor vector $(\rho_1 \ \rho_2 \ \rho_3)^T$ based on the judgements in the matrix is $(0.15 \ 0.51 \ 0.34)^T$. With regard to nodes in disparate WBANs of interfering sources sets, the proposed H guarantees their service quality more thoroughly.

The service order algorithm is described in Algorithm 1 for different nodes in multi-WBANs coexistence scenario. H_m^{start} is the health severity index value of the pending data packet

Algorithm 1 Algorithm for Determining the Service Order of Nodes

---

Input: Physiological data from sensor nodes
Output: Service priority of different data types

1: There are M WBANs in the system while each WBAN has Y sensor nodes.
2: **for** m=1:M **do**
3:     compute H_m according to Eq. 6
4:     sort $H=[H_m] \downarrow$
5:     **if** $H_m^{start} \geq H_{m+1}^{start}$ **then**
6:       serve WBAN m
7:       **for** y=1:Y **do**
8:         compute H_m^y according to Eq. 6
9:         sort $H=[H_m^y] \downarrow$
10:         **if** $H_m^y > H_m^{y+1}$ **then**
11:           serve node y in WBAN m
12:         **else**
13:           serve node $y+1$ in WBAN m
14:         **end if**
15:       **end for**
16:     **end if**
17: **end for**

located at the head of data queue in hub N_{mh}. H_m^y is the health severity index value of node y in WBAN m. According to Eq. 6, the values of health critical index of different WBANs and different nodes could be acquired. Then we sort the WBANs or nodes by the value of H from large to small. Anyone with the higher H value is conferred the higher privilege to access the channel. The introduced H helps to ensure that nodes in emergency condition could be processed in lower delay and better services for health monitoring.

V. PERFORMANCE ANALYSIS

Multiple concurrent WBANs share the same operating channel. Sensors in different WBANs may collide over the channels. We investigate the slow movement scenario. The channel coherence time is relative long. The interference channel gain could be considered unchanged. The channel fading and path loss of the movement is neglected. In this section, we analyze the normalized throughput and average packet delay by employing a three-dimensional Markov model.

A. Superframe Structure

In the light of IEEE 802.15.6, two Exclusive Access Phases (EAPs), two Random Access Phases (RAPs), two Managed Access Phases (MAPs), and a Contention Access Phase (CAP) are placed in order in the superframe. The seven access phases phases are optional. In this paper, only the contention phases EAP and RAP are selected. All the nodes in the network are synchronized to support the contention-based mechanism while the hub establishes the time reference operating in the beacon mode with superframes. Each superframe is bounded by a maximum number of 255 equal length allocation slots. The layout of superframe is shown in Fig. 5.
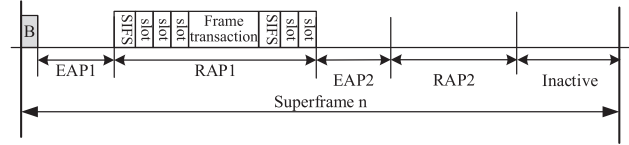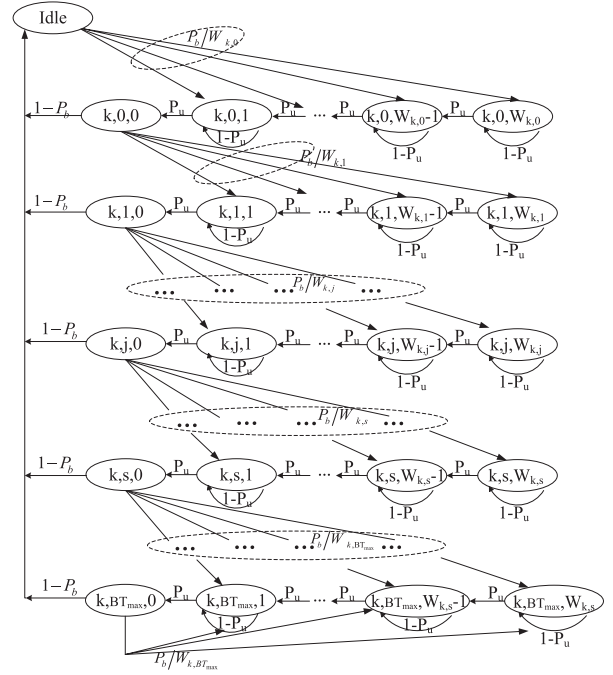

Fig. 5. The superframe structure.

Fig. 6. Markov model for a node with UP_k.

The Beacon (B) frame is transmitted by the hub at the beginning of each superframe to notify network management information such as BAN identification, synchronization and coordination of medium access. If there is highest priority data, the hub and nodes could acquire a contended allocation Short Interframe Space (SIFS) after the beginning of EAP (EAP1 or EAP2) without performing the CSMA/CA. In RAP, all UP_k nodes perform CSMA/CA to contend for available slots to transmit management or data frames. If there are no more pending transmissions in data queues, all nodes including hub turn into inactive state over some time intervals for energy saving.

B. Markov Chain Model for A UP_k Node With Interference

Nodes contend to access the channel in CSMA/CA mechanism for intra-WBAN. In light of the random characteristics of contention progress of the nodes, the access attempts of node having pending data to be transmitted can be analyzed with a three-dimensional discrete time Markov chain. The Markov chain model for the contention progress is shown as Fig. 6. All the notations used in the analysis are presented in Table I.

The state of a node at moment t in the contention progress can be described by three variables $\{k, BT(t), CW(t)\}$, where k is the user priority of a node, BT is the backoff times, and

CW is the contention window value in Backoff Counter (BC). Prioritized access for different types of traffic with different UPs shall be attained through the predefined CW values. The relation between contention window bounds CW_{max} and CW_{min} and the corresponding data traffic is shown in Table II.

Nodes which have data to be transmitted will switch their states between back-off and data transmission, or nodes will turn into inactive state to save energy. At the initial state, a node with user priority k denoted by UP_k senses the channel having been idle for at least a short interframe spacing (pSIFS) time interval. Then it selects a random integer from the interval $[1, CW_{UP_k}]$ as the BC values, where $CW_{UP_k} \in (CW_{\min[UP_k]}, CW_{\max[UP_k]})$. The values of $CW_{\min[UP_k]}$ and $CW_{\max[UP_k]}$ can be obtained from Table II. Furthermore, the BC is decreased by one for each idle CSMA/CA slot, and nodes will switch to transmission state once the BC reaches zero meanwhile the channel is idle. Otherwise, the BC will be locked if the channel is busy or the remaining time interval is not long enough for completing a frame transaction. The BT increases by one in case of an unsuccessful medium access due to collisions. Nodes conduct the backoff progress until the frame is transmitted successfully or initiate a new data transmission when the BT value reaches the maximum backoff retry limits BT_{max}.

We suppose that there are M WBANs in a dense deployment scenario. There are one hub and n_k nodes of UP_k, where $\sum_{k=0}^{7} n_k = Y$, $k = 0, \ldots, 7$, operates in the beacon mode with superframe boundaries in a random selected target WBAN. Assuming that the access probability of node UP_k in a random CSMA/CA slot is τ_k. The access probability of interference nodes is considered sharing the same probability with a UP_k node. The probability that channel is idle during the contention intervals of the target WBAN is

$$P_{idle} = \prod_{k=0}^{7} (1 - \tau_k)^{n_k} \tag{7}$$

The backoff counter is locked when the channel is busy and the remainder time is not long enough completing a frame transaction during its backoff stage. The probabilities that the backoff counter is locked due to the insufficient remaining time for a frame transaction from the current CSMA contended allocation slot to the end of the EAP and RAP period are

$$P_{UP_k-inlock} = \frac{T_R - T_{data} - T_{kCW}}{T_R}, \quad RAP \tag{8}$$

$$P_{UP_7-inlock} = \frac{T_E + T_R - T_{data} - T_{7CW}}{T_E + T_R}, \quad EAP \ and \ RAP \tag{9}$$

where T_E and T_R is the number of CSMA slots allocated to UP_k in EAP and RAP access phases, respectively. T_{data} is the successful data transmission time. The backoff times is marked as l and the mean backoff value is approximately calculated as $\frac{CW_{\min[UP_k]} + CW_{\max[UP_k]}}{4}$ [31]. T_{kCW} is the backoff time and

can be calculated as

$$T_{kCW} = \sum_{l=0}^{BT_{max}} \frac{T_{c-slot}\left(CW_{\min[UP_k]} + CW_{\max[UP_k]}\right)}{4} \tag{10}$$

$$T_{c-slot} = T_{CCA} + T_{MP} \tag{11}$$

where T_{c-slot} is the CSMA slot length with a fixed duration. T_{CCA} is the Clear Channel Assessment (CCA) time and T_{MP} is the time cost that MAC transfers a frame to the Physical (PHY) layer.

For the highest user priority data, the contention attempts are exclusively allowed in EAP. A hub or a node may regard the combined EAP (EAP1 or EAP2) and RAP (RAP1 or RAP2) as a single EAP1 or EAP2 to allow continual invocation of CSMA/CA and improve channel utilization. Therefore, the probability of the channel is idle for UP_7 in a CSMA slot during EAP and RAP is different [49]. The idle channel probability P_{7idle} of UP_7 node in EAP and RAP can be obtained from Eq. (12). Then the random selected UP_7 node lock its backoff counter owing to the busy channel can be obtained from $P_{7b} = 1 - P_{7idle}$.

$$P_{7idle} = \frac{T_E(1-\tau_7)^{n_{7I}+n_7-1}}{T_E + T_R} + \frac{T_R P_{idle}(1-\tau_7)^{n_{7I}-1}}{T_E + T_R} \tag{12}$$

where n_{7I} is the number of interference nodes with UP_7 from inter-WBANs. The value of n_{7I} can be obtained from Eq. (5). n_7 is the number of UP_7 nodes from intra-WBAN. P_{idle} is the probability that channel is idle during the contention intervals of the target WBAN.

In RAP, a node with UP_k locks its backoff counter when it finds the channel is busy in its backoff counter countdown. In other words, at least one of the remaining nodes of intra-WBAN or interference nodes of inter-WBAN sends packets or ACK packets, leading to the collision. There are n_{kI} interference sources from inter-WBAN affecting the data transactions. Supposing that the node finds the channel is idle in probability P_{kidle} during its backoff period, the P_{kidle} is described as

$$P_{kidle} = \frac{(1-\tau_k)^{n_{kI}+n_k} \prod_{i \neq k} (1-\tau_i)^{n_i}}{(1-\tau_k)}$$

$$= (1-\tau_k)^{n_{kI}-1} \prod_{i=0}^{7} (1-\tau_k)^{n_k} \tag{13}$$

The packet collision probability P_b for each UP_k node at any backoff stage equals the probability of busy channel and could be expressed as

$$P_b = 1 - P_{kidle} = 1 - (1-\tau_k)^{n_{kI}-1} \prod_{i=0}^{7} (1-\tau_k)^{n_k} \tag{14}$$

According to Eq. (7)-Eq. (14), the probability P_u that the backoff counter is unlock can be obtained in Eq. (15). Eq. 15 (a) is particularly for UP_7 nodes to get the unlocked probability in EAP and RAP. The probability of the other $UP_k(k = 0, \ldots, 6)$ data unlock its back counter in RAP is

indicated in Eq. 15 (b).

$$P_u = (1 - P_b)(1 - P_{UP_k - inlock})$$

$$= \begin{cases} P_{7idle}(\dfrac{T_{data} + T_{CW}}{T_E + T_R}), & (a) \\ P_{kidle}(1 - \tau_k)^{n_I - 1}\left(\dfrac{T_{data} + T_{kCW}}{T_R}\right), & (b) \end{cases} \quad (15)$$

If the collision occurs, the node resets the CW value of backoff counter according the regulations aforementioned, selects a random integer from the interval $[1, CW_{UP_k}]$ and turns into the next backoff stage. Thereafter, the changing CW_{UP_k} value $W_{k,j}$ during the jth backoff period for a node of UP_k is predicted as following,

$W_{k,0} = CW_{\min[UP_k]}, j = 0$

$W_{k,j} = W_{k,j-1}$, for j is an odd number, $1 \le j \le BT_{max}$

$W_{k,j} = \min\{2W_{k,j-1}, CW_{\max[UP_k]}\}$, for j is an even number, $1 < j \le BT_{max}$

The first time CW value reaches $CW_{\max[UP_k]}$ at its sth backoff stage and remains unchanged in the following backoff retry procedure. The stationary distribution probability of the Markov chain is $M_{k,j,i}$, where k is the user priority ($k = 0, \ldots, 7$), j is the value of back off stages ($j = 0, 1, \ldots, BT_{max}$), and i is the BC values ($i = 0, 1 \ldots, W_{k,j}$). The state transition probabilities are given by

$$P\{k, j+1, W_{k,j} | k, j, 0\} = \frac{P_b}{W_{k,j}}, \forall j \in [0, BT_{max} - 1] \quad (16)$$

$$P\{k, j+1, 0 | k, j, 0\} = P_b \quad (17)$$

$$P\{k, j, W_{k,j} - 1 | k, j, W_{k,j}\} = P_u \quad (18)$$

$$P\{k, j, W_{k,j} | k, j, W_{k,j}\} = 1 - P_u \quad (19)$$

Nodes will discard the packet if the packet fails in accessing the channel. The failure data transmission probability P_f of UP_k node is expressed as

$$P_f = P_b^{BT_{max}+1} \quad (20)$$

In steady state, we can get the following relations according to the Markov chain regularities. Eq. (25) shows the sum of all the state probabilities is equal to one.

$$M_{k,j,0} = P_b^j M_{k,0,0}, \ \forall j \in [0, BT_{max}] \quad (21)$$

$$M_{k,BT_{max},0} = \frac{P_b^{BT_{max}}}{1 - P_b} M_{k,0,0} \quad (22)$$

$$M_{0,0,0} = \frac{P_b}{1 - P_b} M_{k,0,0} \quad (23)$$

$$M_{k,j,i} = \frac{W_{k,j} - i + 1}{W_{k,j} P_u} M_{k,j,0}, i \in [1, W_{k,j}] \quad (24)$$

$$1 = M_{0,0,0} + \sum_{j=0}^{BT_{max}} \sum_{i=0}^{W_{k,j}} M_{k,j,i} \quad (25)$$

All the probabilities have a strong correlation with access probability τ. Once the value of backoff counter is zero, the node initiates an attempt to access the channel. Therefore, the access probability of node UP_k in a random CSMA slot τ_k is the sum all the steady states probabilities $\tau_k = \sum_{j=0}^{BT_{max}} M_{k,j,0}$.

C. Normalized Throughput and Average Access Delay

We define the normalized throughput as the ratio of time cost of average successful transmitted payloads to the total intervals between two consecutive transmissions. A successful packet transmission time is T_{pk} and can be obtained from

$$T_{pk} = \frac{N_{packet}}{R_s}$$

$$= \frac{N_{preamble} + N_{header} \times S_{header} + \frac{N_{total} \times S_{PSDU}}{\log_2 M}}{R_s} \quad (26)$$

where R_s is the sysmbol rate. $N_{preamble}$ and N_{header} stand for the length of Physical Layer Convergence Protocol (PLCP) preamble and header, respectively. S_{header} denotes the spreading factor for the PLCP header. S_{PSDU} denotes the spreading factor for Physical Service Data Unit (PSDU). M is the cardinality of the constellation of a given modulation scheme. N_{total} is the total bits which flow in the PHY layer and can be derived in Eq. 27.

$$N_{total} = N_{PSDU} + \log_2 M \left\lceil \frac{N_{PSDU} + (n-k)N_{CW}}{\log_2 M} \right\rceil$$
$$+ (n-k)N_{CW} - [N_{PSDU} + (n-k)N_{CW}] \quad (27)$$

where N_{CW} denotes the number of Bose, Ray-Chaudhuri, Hocquenghem code (BCH) codewords in a frame. In IEEE 802.15.6, $N_{CW} = \left\lceil \frac{N_{PSDU}}{k} \right\rceil$, where n and k are selected by BCH encoder to achieve the desired code rate k/n. N_{PSDU} is the length of the PSDU. This component is formed by concatenating the MAC header with the MAC payload and frame check sequence (FCS). Given the length of MAC header $N_{MHeader}$, MAC payload $N_{MPayload}$ and FCS N_{FCS}, the N_{PSDU} can be acquired from Eq. (28).

$$N_{PSDU} = 8 \times (N_{MHeader} + N_{MPayload} + N_{FCS}) \quad (28)$$

$$T_{MPayload} = \frac{N_{MPayload} \times S_{PSDU}}{\log_2 M \times R_s} \quad (29)$$

The normalized throughput with the interference is calculated as

$$S_k = \frac{\tau_k P_{kidle} T_{MPayload}}{P_{idle} T_{c-slot} + \tau_k P_{kidle} T_{pk} + \tau_k (1 - P_{kidle}) T_{fpk}} \quad (30)$$

where T_{c-slot} is the contended CSMA/CA slot length. P_{kidle} is the probability that the channel is idle during the backoff period of node UP_k. P_{kidle} is influenced by the number of interfering nodes, the value of which can be obtained from Eq. (12) and Eq. (13). T_s in Eq. (31) is the mean time of a successful transmission.

$$T_s = T_{pk} + T_{pSIFS} + T_{I-ACK} \quad (31)$$

While the occupied slot length for a failure packet delivery T_{fpk} is described as

$$T_{fpk} = T_{pk} + T_{pSIFS} + T_{timeout} \quad (32)$$

An absent I-ACK in an interval $T_{timeout}$ will be treated as a failure transmission. The T_{fail} is the total time cost before a packet has been successfully transmitted.

$$T_{fail} = \sum_{l=0}^{BT_{max}} lP_b^l (T_{pk} + T_{pSIFS} + T_{timeout}) + T_{kCW} \quad (33)$$

TABLE V

SYSTEM PARAMETERS

Parameters	Values	Parameters	Values
Superframe length	1 s	Beacon	15 bytes
CSMA slot length	145 μs	FCS	2 bytes
pAllocationSlotMin	500 μs	L	7
pAllocationResolution	500 μs	M	4
Max BAN Size	64	S_{PSDU}	1
MAC header	7 bytes	S_{header}	4
PLCP preamble	90 bits	pCCA time	105 μs
PLCP header	31 bits	pMIFS	20 μs
Symbol rate	600 ksps	pSIFS	75 μs
Buffer size	20000 bytes	Coderate(k/n)	51/63
Frequency band	2400-2438.5 MHz	Timeout	30 μs

where l is the failure times before the packet is successfully transmitted. The average packet delay is defined as the time interval from the packet that is ready to be transmitted to the moment that the I-ACK frame of this packet is received. In Eq. (34), the average delay D_k is given as

$$D_k = T_s + T_{fail} \tag{34}$$

By substituting Eqs. (31) and (33) into Eq. (34), the average access delay can be calculated. Both the normalized throughput and the average access delay consider the traffic differentiation and interference dynamics.

VI. PERFORMANCE EVALUATION

In this section, we evaluate the normalized throughput and the average access delay of coexisting WBANs based on IEEE 802.15.6 CSMA/CA mechanism. Numerical results of the performance evaluation based on the proposed interference model are implemented and verified by the simulation tool MATLAB. One-hop star topology structure in a WBAN is considered in the monitoring scenario. The channel fading and path loss of the movement could be neglected in slow movements. The channel condition is ideal during the data transmission. Each hub operates in the beacon mode with superframes and each node produces one UP traffic in the network with all the data fluctuation in normal range. The health critical index value H is in corresponding to their UP values of each node. The length of an allocation slot T_{slot} is equal to $pAllocationSlotMin + L \times pAllocationSlotResolution$ [15]. The maximum MAC payload size is 250 bytes in the analysis. The other relevant simulation parameters are listed in Table V.

A. Normalized Throughput

The normalized throughput of the nodes with user priorities varying from 0 to 7 are shown in Fig. 7- Fig. 9. At first, we evaluate the normalized throughput of nodes with no interference. In other words, there is no other coexisting WBANs in the communication range of the target WBAN N_1. The relationship between normalized throughput and the varied payloads is shown in Fig. 7. There are 8 sensor nodes except the hub in the network. It is obvious that the normalized throughput of UP_k node increases as the payload increases and the UP_7 node increases faster than any other nodes. The reason
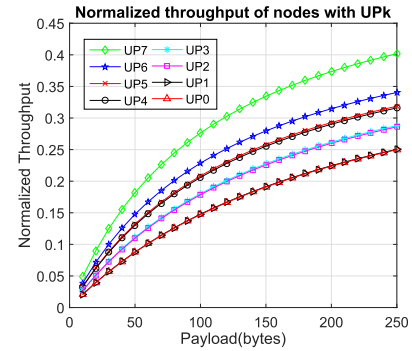

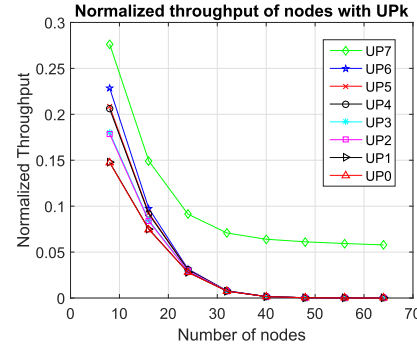Fig. 7. Normalized throughput versus payloads.

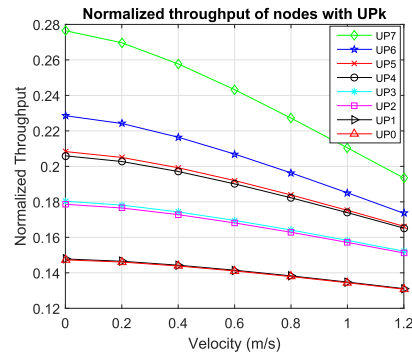Fig. 8. Normalized throughput versus number of nodes.

Fig. 9. Normalized throughput versus velocity.

is that the nodes with highest user priority traffic can transmit data in the EAP period and RAP period. Moreover, UP_7 node enjoys a smallest contention window value and has a higher access probability as well as lower collision probability than any other nodes in the CSMA/CA period. We can see that the normalized throughput of UP_5 and UP_4 nodes, UP_3 and UP_2 nodes, UP_1 and UP_0 nodes almost have the same tendency while the payload increases. This is because some of them share the same minimum contention window value and have small difference in access probability.

Fig. 8 describes the relationship between normalized throughout and the number of nodes with a payload of 100 bytes and there is no interfering nodes. As the number of nodes in the network increases to the maximum WBAN size, i.e. 64 sensor nodes in a WBAN, the normalized throughput suffers a sharply decrease. Especially when the number
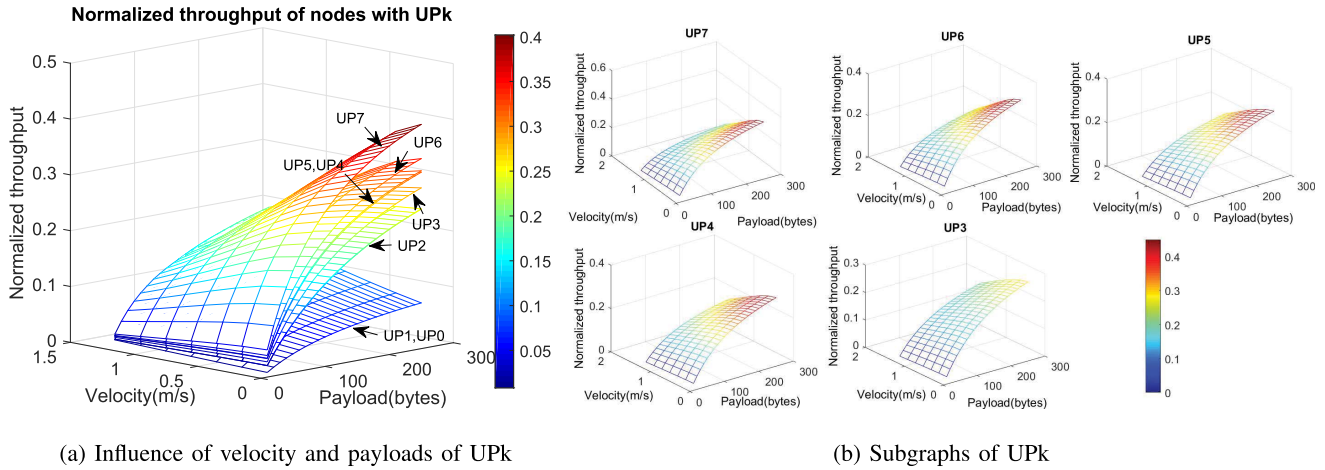
(a) Influence of velocity and payloads of UPk

(b) Subgraphs of UPk

Fig. 10. Normalized throughput versus velocity and payloads.

(a) Influence of velocity and number of nodes
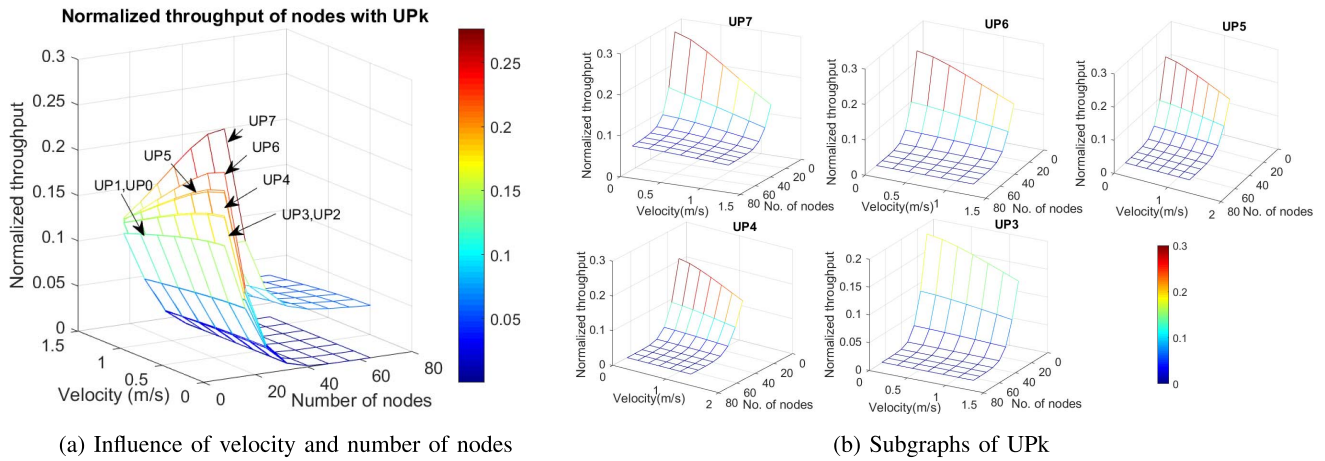
(b) Subgraphs of UPk

Fig. 11. Normalized throughput versus and velocity and number of nodes.

of nodes is more than 40 in the network, the normalized throughput of UP_k nodes (except UP_7 nodes) is almost zero. All this is owing to the high collision probability of increasing number of nodes. Although in such a condition, the highest priority UP_7 node can still transmit data in the particular EAP period, contending to access the channel with few UP_7 traffic data. The QoS of nodes with the higher user priority can be guaranteed. The number of nodes really has a big influence on the normalized throughput. It is suggested that the number of nodes in one WBAN is better no more than 24 from Fig. 8.

We investigate how a random mobile WBAN N_m affects the performance of target WBAN N_1 on normalized throughput in Fig. 9. There are 8 nodes with payload of 100 bytes in target WBAN N_1. The communication range of N_1 is 1.5 m. The movement of N_m does not affect the performance of N_1 when the inter-WBAN distance is large than 3 m. The velocity of N_m regards zero to N_1. When the inter-WBAN distance is equal to or less than 3 m, the N_m becomes interference source. We focus on the slow motion of patients or old people in health monitoring. N_m keeps in slow linear motion towards to N_1 during the interference duration. Within the specific time, the velocity of N_m generates varying interference dynamics. The normalized throughput of UP_k nodes

in N_1 decrease with the increasing velocity of N_m. The normalized throughput variation of high UP node is larger than lower UP node. The normalized throughput of UP_7 decreases almost 32% when N_m moves to N_1 at the speed 1.2m/s. The higher user priority nodes have higher access probability and suffer higher collision probability with the increasing interference.

The impacts of velocity combined the effects of payloads and number of nodes acting together on normalized throughput of UP_k nodes are shown in Fig. 10 and Fig. 11, respectively. The comparison of normalized throughput of different user priority traffic varieties is obvious. The normalized throughput of UP_k nodes increases with the payloads increasing, and decreases with the increasing velocity. UP_7 traffic always has highest throughput while UP_0 has the lowest throughput. The normalized throughput of several typical user priority are shown in Fig. 10 (b) and Fig. 11 (b). The normalized throughput is affected greater by the number of nodes in the network than the velocity parameter in Fig. 11. The variation of velocity means the varying number of interference nodes in the network, which seriously affects higher UPs. Once the number of nodes in the WBAN is larger than 40, the packets can hardly be transmitted successfully.
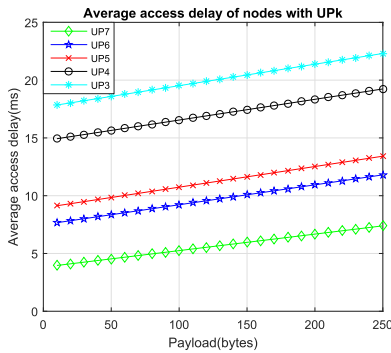
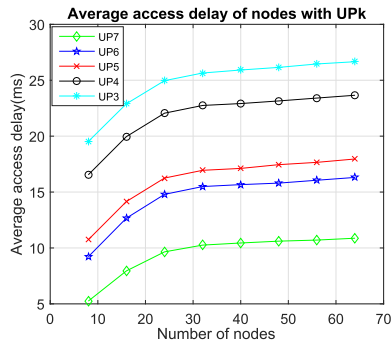Fig. 12. Average access delay versus payloads.

Fig. 13. Average access delay versus number of nodes.

Fig. 14. Average access delay versus velocity.

B. Average Access Delay

The variations of average packet access delay against the payloads for different UPs with no interference are shown in Fig. 12. We choose the typical $UP_k(k = 3, \ldots, 7)$ nodes to illustrate the results. The results of all the UP_k nodes can be found in Fig. 15 and Fig. 16. The delay increases as the length of payloads increases. In this case, only 8 nodes are considered in a WBAN. Every node produces one kind of user priority data. The higher UP of the node is, the lower access delay is. In the maximum payload 250 bytes, the delay of UP_7 node is merely ninth of the UP_0 node, and is only 62% of the UP_6 node. The reason is that nodes with higher UPs have higher packet transmission probability compared to nodes with lower UPs.

The delay of nodes increases with the increasing number of nodes in the network, as shown in Fig. 13. All the nodes are in a fixed payload (100 bytes). Nodes have to back off more times in a successful data transmission with the increasing number of nodes in the network. The access probabilities of all UP_k nodes become smaller with the increasing number of nodes, leading to the increasing delay. As the number of nodes increases from 8 to 32, the access delay of UP_7 have doubled, and the delay of UP_6 increases 70%, while the growth of UP_5 and UP_4 is 60% and 38%, respectively. If there are too many nodes in a WBAN, all nodes suffer a severe contention progress and very high average access delay.

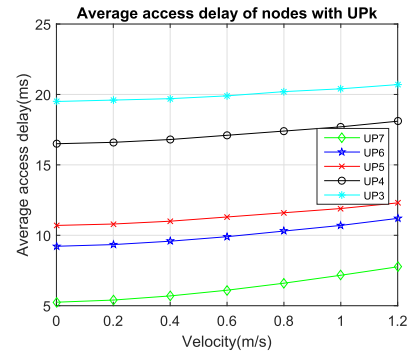The average access delay of the target WBAN N_1 increases with the increasing velocity of neighbor interference WBAN N_m. The higher velocity of N_m within the specific time makes more nodes in N_m become interference nodes to N_1. Fig. 14 shows impacts of interference nodes on the average access delay of UP_k nodes. The UP_7 nodes with no interference cost less than 70% time of N_m in walking motion. The average access delay of UP_k nodes increases with the increasing interference nodes due to the changing velocity. The reason is that the nodes have to suffer a relative long back-off procedure.

The combined action of velocity and different length of payloads on average access delay are shown in Fig. 15. All the nodes are in normal states that there is no dramatic shift on the monitoring data. The delay increases as the length of payloads increases and higher UP nodes have lower delay. The UP_7 always has the lowest delay while UP_0 always has the highest delay. The reason is that nodes with higher UPs have higher packet transmission probability compared to nodes with lower UPs. From Fig. 15 (b), we can see that the delay is much influenced by the payload when it is larger than 100 bytes. The varying velocity of neighbor WBAN makes little effect on the average access delay of UP_k nodes in the target WBAN in spite of the changing length of payloads.

The average access delay of the IEEE 802.15.6 based CSMA/CA protocol for different UP nodes by considering the interference of coexisting mobile neighbour WBAN and the different number of nodes in intra-WBAN are shown in Fig. 16 (a) and (b). The network performance on delay is severely deteriorated when the number of nodes increases, since the packet collision happens not only among nodes with different UPs but also among nodes with same UPs. The higher UPs are more sensitive to the collision due to the high access probability. Though the UP_7 nodes are more volatile than any other UP nodes when the number of nodes and the velocity of neighbor WBAN changes, the average access delay of UP_7 nodes is the lowest in the same condition. The delay of UP_3 is almost two to three times as the delay of UP_7 nodes in different number of nodes at the same velocity. To guarantee the monitoring data be transmitted in time, the number of nodes in one WBAN had better not exceed 30.

Human movements lead to the increasing number of interfering WBANs and interfering nodes, which increases the collision probability of nodes accessing the channel. The impacts of dynamic mobility with different number of coexisting WBANs on the normalized throughput and average access
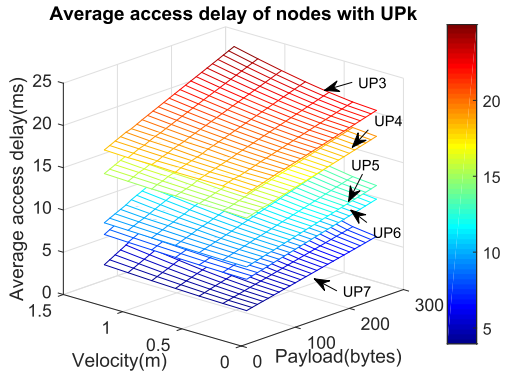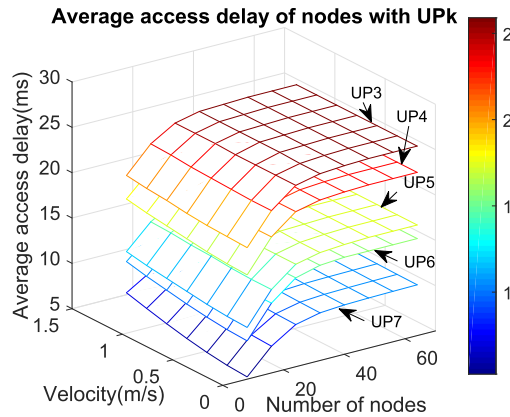
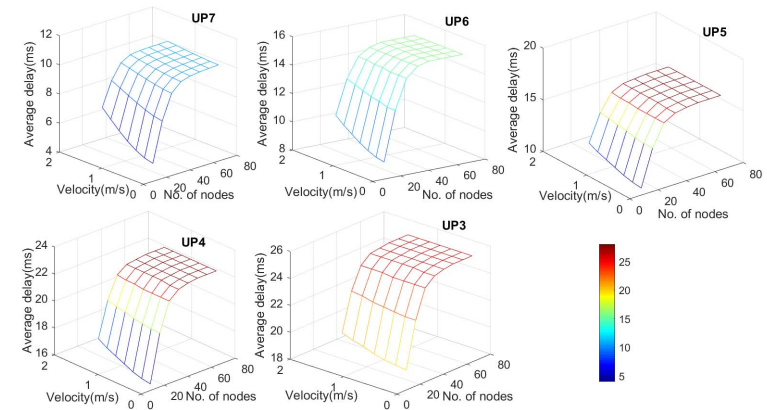(a) Influence of velocity and payloads of UPk
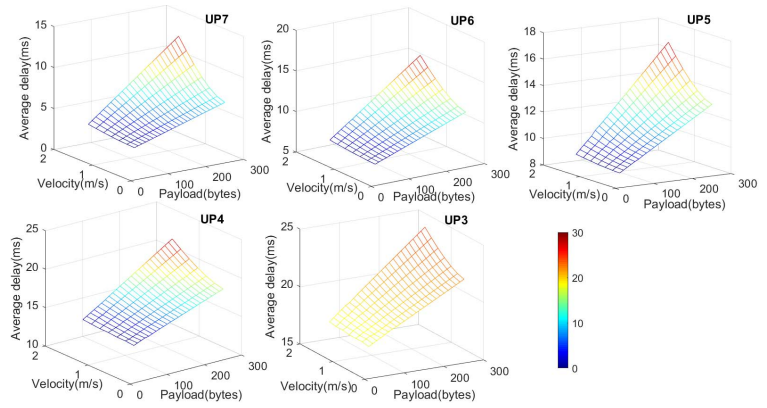
(b) Subgraphs of UPk

Fig. 15.   Average access delay versus velocity and payloads.

(a) Influence of velocity and number of nodes

(b) Subgraphs of UPk

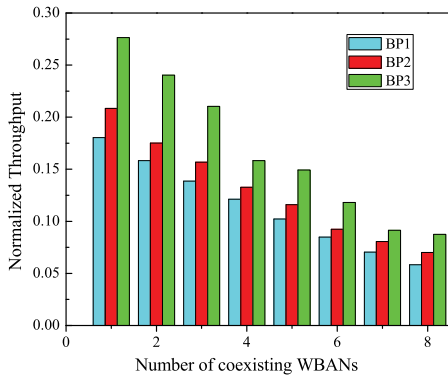Fig. 16.   Average access delay versus velocity and number of nodes.

Fig. 17.   Normalized throughput versus number of coexisting WBANs.
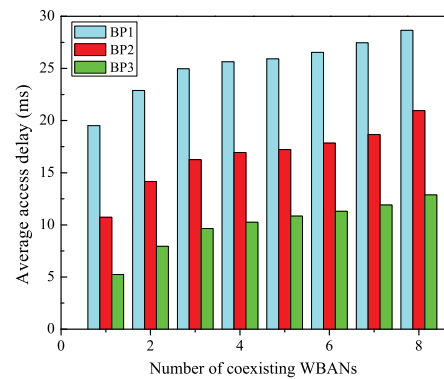

Fig. 18.   Average access delay versus number of coexisting WBANs.

delay are reflected in Fig. 17 and Fig. 18. The performance of UP_7 node in target WBAN is evaluated with different WBAN priorities. The $BP3$, $BP2$ and $BP1$ make the target WBAN in highest, moderate and low health critical index among the coexisting WBANs, respectively. The normalized throughput decreases 70% while the average access delay is doubled compared with single WBAN. The higher WBAN priority guarantees the node in higher normalized throughput and

lower average access delay with the increasing interference. The evaluation results in Fig. 17 and Fig. 18 facilitate the network configuration and optimization in WBAN coexistence scenario.

VII. CONCLUSION

In this paper, we have analyzed the dynamic interference generated by varying number of interfering nodes from

neighbour WBANs owing to human mobility in multi-WBAN coexistence scenario. We have developed a three dimensional Markov chain model to investigate the interference dynamics on network performance of IEEE 802.15.6-based CSMA/CA protocol. Moreover, a health critical index considering the data traffic differentiate, data severity and WBANs priority has been designed to guarantee the emergency data taking precedence over general traffic to access the channel with lower delay and high reliability. The normalized throughput and average access delay under different interference conditions have been derived in tractable expressions. The appropriate number of nodes in a WBAN and distance to the nearby WBANs could be acquired according to the analytical results, which is useful to network configuration and interference mitigation. In the future, we will consider the dynamic channel status in different movement manners and analyze the impacts on network performance. The interference mitigation schemes are also scheduled in WBANs coexistence.

REFERENCES

[1] R. Chavez-Santiago *et al.*, "Propagation models for IEEE 802.15.6 standardization of implant communication in body area networks," *IEEE Commun. Mag.*, vol. 51, no. 8, pp. 80–87, Aug. 2013.

[2] K. Zhang, K. Yang, X. Liang, Z. Su, X. Shen, and H. H. Luo, "Security and privacy for mobile healthcare networks: From a quality of protection perspective," *IEEE Wireless Commun.*, vol. 22, no. 4, pp. 104–112, Aug. 2015.

[3] A. Al-Fuqaha, M. Guizani, M. Mohammadi, M. Aledhari, and M. Ayyash, "Internet of things: A survey on enabling technologies, protocols, and applications," *IEEE Commun. Surveys Tuts.*, vol. 17, no. 4, pp. 2347–2376, 4th Quart., 2015.

[4] Q. Ye and W. Zhuang, "Distributed and adaptive medium access control for Internet-of-Things-enabled mobile networks," *IEEE Internet Things J.*, vol. 4, no. 2, pp. 446–460, Apr. 2017.

[5] Q. Ye, W. Zhuang, L. Li, and P. Vigneron, "Traffic-load-adaptive medium access control for fully connected mobile ad hoc networks," *IEEE Trans. Veh. Technol.*, vol. 65, no. 11, pp. 9358–9371, Nov. 2016.

[6] X. Wu, Y. I. Nechayev, C. C. Constantinou, and P. S. Hall, "Interuser interference in adjacent wireless body area networks," *IEEE Trans. Antennas Propag.*, vol. 63, no. 10, pp. 4496–4504, Oct. 2015.

[7] X. Wang and L. Cai, "Interference analysis of co-existing wireless body area networks," in *Proc. IEEE GLOBECOM*, Houston, TX, USA, Dec. 2011, pp. 1–5.

[8] Z. Zhang, H. Wang, C. Wang, and H. Fang, "Interference mitigation for cyber-physical wireless body area network system using social networks," *IEEE Trans. Emerg. Topics Comput.*, vol. 1, no. 1, pp. 121–132, Jun. 2013.

[9] T. T. T. Le and S. Moh, "Interference mitigation schemes for wireless body area sensor networks: A comparative survey," *Sensors*, vol. 15, no. 6, pp. 13805–13838, 2015.

[10] L. Zou, B. Liu, C. Chen, and C. W. Chen, "Bayesian game based power control scheme for inter-WBAN interference mitigation," in *Proc. IEEE GLOBECOM*, San Diego, CA, USA, Dec. 2015, pp. 240–245.

[11] S. Kim, S. Kim, J.-W. Kim, and D.-S. Eom, "A beacon interval shifting scheme for interference mitigation in body area networks," *Sensors*, vol. 12, no. 8, pp. 10930–10946, 2012.

[12] S. Kim, S. Kim, J.-W. Kim, and D.-S. Eom, "Flexible beacon scheduling scheme for interference mitigation in body sensor networks," in *Proc. IEEE SECON*, Seoul, South Korea, Jun. 2012, pp. 157–164.

[13] A. Meharouech, J. Elias, and A. Mehaoua, "Future body-to-body networks for ubiquitous healthcare: A survey, taxonomy and challenges," in *Proc. Int. Symp. Ubi-HealthTech*, Beijing, China, May 2015, pp. 1–6.

[14] X. Yuan *et al.*, "Dynamic interference analysis of coexisting mobile WBANs for health monitoring," in *Proc. IEEE ICC*, Kansas City, MO, USA, May 2018, pp. 1–6.

[15] *IEEE Standard for Local and Metropolitan Area Networks—Part 15.6: Wireless Body Area Networks*, IEEE Standard 802.15.6-2012, IEEE Standards Association, 2012, pp. 1–271.

[16] A. Samanta and S. Misra, "Energy-efficient and distributed network management cost minimization in opportunistic wireless body area networks," *IEEE Trans. Mobile Comput.*, vol. 17, no. 2, pp. 376–389, Feb. 2018.

[17] Y. Hou, M. Li, and S. Yu, "Making wireless body area networks robust under cross-technology interference," *IEEE Trans. Wireless Commun.*, vol. 16, no. 1, pp. 429–440, Jan. 2017.

[18] S. Marwa, A.-D. Ahmed, R. Imed, and N. Youssef, "Wireless body area network (WBAN): A survey on reliability, fault tolerance, and technologies coexistence," *ACM Comput. Surv.*, vol. 50, no. 1, 2017, Art. no. 3.

[19] W. Sun, Y. Ge, and W.-C. Wong, "A stochastic geometry analysis of inter-user interference in IEEE 802.15.6 body sensor networks," in *Proc. IEEE WCNC*, New Orleans, LA, USA, Mar. 2015, pp. 1912–1917.

[20] F. Jameel, A. Butt, and U. Munir, "Analysis of interference in body area networks over generalized fading," in *Proc. IEEE ICET*, Islamabad, Pakistan, Oct. 2016, pp. 1–6.

[21] M. N. Anjum and H. Wang, "Optimal resource allocation for deeply overlapped self-coexisting WBANs," in *Proc. IEEE GLOBECOM*, Washington, DC, USA, Dec. 2016, pp. 1–7.

[22] J. Elias, S. Paris, and M. Krunz, "Cross-technology interference mitigation in body area networks: An optimization approach," *IEEE Trans. Veh. Technol.*, vol. 64, no. 9, pp. 4144–4157, Sep. 2015.

[23] *IEEE Standard for Local and Metropolitan Area Networks—Part 15.4: Low-Rate Wireless Personal Area Networks (LR-WPANs)*, IEEE Standard 802.15.4, IEEE Computer Society, Sep. 2011.

[24] K. Zhang, X. Liang, M. Baura, R. Lu, and X. Shen, "PHDA: A priority based health data aggregation with privacy preservation for cloud assisted WBANs," *Inf. Sci.*, vol. 284, pp. 130–141, Nov. 2014.

[25] W. Sun, Y. Ge, Z. Zhang, and W.-C. Wong, "An analysis framework for interuser interference in IEEE 802.15.6 body sensor networks: A stochastic geometry approach," *IEEE Trans. Veh. Technol.*, vol. 65, no. 10, pp. 8567–8577, Oct. 2016.

[26] X. Cao, J. Chen, Y. Cheng, X. S. Shen, and Y. Sun, "An analytical MAC model for IEEE 802.15.4 enabled wireless networks with periodic traffic," *IEEE Trans. Wireless Commun.*, vol. 14, no. 10, pp. 5261–5273, Oct. 2015.

[27] G. Bianchi, "Performance analysis of the IEEE 802.11 distributed coordination function," *IEEE J. Sel. Areas Commun.*, vol. 18, no. 3, pp. 535–547, Mar. 2000.

[28] S. Moulik, S. Misra, and D. Das, "AT-MAC: Adaptive MAC-frame payload tuning for reliable communication in wireless body area networks," *IEEE Trans. Mobile Comput.*, vol. 16, no. 6, pp. 1516–1529, Jun. 2017.

[29] P. Park, P. Di Marco, C. Fischione, and K. H. Johansson, "Modeling and optimization of the IEEE 802.15.4 protocol for reliable and timely communications," *IEEE Trans. Parallel Distrib. Syst.*, vol. 24, no. 3, pp. 550–564, Mar. 2013.

[30] S. Sarkar, S. Misra, B. Bandyopadhyay, C. Chakraborty, and M. S. Obaidat, "Performance analysis of IEEE 802.15.6 MAC protocol under non-ideal channel conditions and saturated traffic regime," *IEEE Trans. Comput.*, vol. 64, no. 10, pp. 2912–2925, Oct. 2015.

[31] S. Rashwand, J. Mišić and V. B. Mišić, "Analysis of CSMA/CA mechanism of IEEE 802.15.6 under non-saturation regime," *IEEE Trans. Parallel Distrib. Syst.*, vol. 27, no. 5, pp. 1279–1288, May 2016.

[32] M. Salayma, A. Al-Dubai, I. Romdhani, and Y. Nasser, "New dynamic, reliable and energy efficient scheduling for wireless body area networks (WBAN)," in *Proc. IEEE ICC*, Paris, France, May 2017, pp. 1–6.

[33] D.-R. Chen, "A QoS bandwidth allocation method for coexistence of wireless body area networks," in *Proc. PDP*, St. Petersburg, Russia, Mar. 2017, pp. 251–254.

[34] G.-T. Chen, W.-T. Chen, and S.-H. Shen, "2L-MAC: A MAC protocol with two-layer interference mitigation in wireless body area networks for medical applications," in *Proc. IEEE ICC*, Sydney, NSW, Australia, Jun. 2014, pp. 3523–3528.

[35] G. R. Tsouri, S. R. Zambito, and J. Venkataraman, "On the benefits of creeping wave antennas in reducing interference between neighboring wireless body area networks," *IEEE Trans. Biomed. Circuits Syst.*, vol. 11, no. 1, pp. 153–160, Feb. 2017.

[36] S. H. Cheng and C. Y. Huang, "Coloring-based inter-WBAN scheduling for mobile wireless body area networks," *IEEE Trans. Parallel Distrib. Syst.*, vol. 24, no. 2, pp. 250–259, Feb. 2013.

[37] L. Wang, C. Goursaud, N. Nikaein, L. Cottatellucci, and J. M. Gorce, "Cooperative scheduling for coexisting body area networks," *IEEE Trans. Wireless Commun.*, vol. 12, no. 1, pp. 123–133, Jan. 2013.

[38] Y. Tselishchev, A. Boulis, and L. Libman, "Variable scheduling to mitigate channel losses in energy-efficient body area networks," *Sensors*, vol. 12, no. 11, pp. 14692–14710, 2012.

[39] W. Huang and T. Q. Quek, "Adaptive CSMA/CA MAC protocol to reduce inter-WBAN interference for wireless body area networks," in *Proc. IEEE BSN*, Cambridge, MA, USA, Jun. 2015, pp. 1–6.

[40] D. B. Smith, D. Miniutti, T. A. Lamahewa, and L. W. Hanlen, "Propagation models for body-area networks: A survey and new outlook," *IEEE Antennas Propag. Mag.*, vol. 55, no. 5, pp. 97–117, Oct. 2013.

[41] D. B. Smith and L. W. Hanlen, "Channel modeling for wireless body area networks," in *Ultra-Low-Power Short-Range Radios*. Cham, Switzerland: Springer, 2015, pp. 25–55.

[42] S. V. Roy *et al.*, "Dynamic channel modeling for multi-sensor body area networks," *IEEE Trans. Antennas Propag.*, vol. 61, no. 4, pp. 2200–2208, Apr. 2013.

[43] L. Hanlen, D. Miniutti, D. Smith, D. Rodda, and B. Gilbert, "Co-channel interference in body area networks with indoor measurements at 2.4 GHz: Distance-to-interferer is a poor estimate of received interference power," *Int. J. Wireless Inf. Netw.*, vol. 17, nos. 3–4, pp. 113–125, 2010.

[44] S. Misra, S. Moulik, and H.-C. Chao, "A cooperative bargaining solution for priority-based data-rate tuning in a wireless body area network," *IEEE Trans. Wireless Commun.*, vol. 14, no. 5, pp. 2769–2777, May 2015.

[45] S. Moulik, S. Misra, C. Chakraborty, and M. S. Obaidat, "Prioritized payload tuning mechanism for wireless body area network-based healthcare systems," in *Proc. IEEE GLOBECOM*, San Diego, CA, USA, Feb. 2015, pp. 2393–2398.

[46] X. Yuan, C. Li, L. Yang, W. Yue, B. Zhang, and S. Ullah, "A token-based dynamic scheduled MAC protocol for health monitoring," *EURASIP J. Wireless Commun. Netw.*, vol. 2016, no. 1, p. 125, Dec. 2016.

[47] T. L. Saaty, "Decision making with analytic hierarchy process," *Int. J. Services Sci.*, vol. 1, no. 1, pp. 83–98, 2008.

[48] S. Roy, I. Mallik, and S. Moulik, "PAG-MAC: Prioritized allocation of GTSs in IEEE 802.15.4 MAC protocol—A dynamic approach based on analytic hierarchy process," in *Proc. IEEE INDICON*, IIT Roorkee, India, Dec. 2017, pp. 1–5.

[49] S. Rashwand and J. Mišić, "Effects of access phases lengths on performance of IEEE 802.15.6 CSMA/CA," *Comput. Netw.*, vol. 56, no. 12, pp. 2832–2846, 2012.
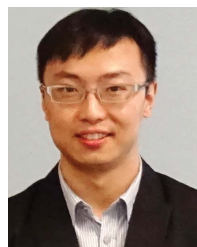
Qiang Ye (S'16–M'17) received the B.S. degree in network engineering and the M.S. degree in communication and information systems from the Nanjing University of Posts and Telecommunications, China, in 2009 and 2012, respectively, and the Ph.D. degree in electrical and computer engineering from the University of Waterloo, Waterloo, ON, Canada, in 2016. He has been a Post-Doctoral Fellow with the Department of Electrical and Computer Engineering, University of Waterloo, since 2016. His current research interests include software-defined networking and network function virtualization, network slicing for 5G networks, virtual network function chain embedding and end-to-end performance analysis, medium access control and performance optimization for mobile ad hoc networks, and the Internet of Things.

Kuan Zhang (S'13–M'17) received the B.Sc. degree in communication engineering and the M.Sc. degree in computer applied technology from Northeastern University, China, in 2009 and 2011, respectively, and the Ph.D. degree in electrical and computer engineering from the University of Waterloo, Canada, in 2016. He was a Post-Doctoral Fellow with the Broadband Communications Research Group, Department of Electrical and Computer Engineering, University of Waterloo, Canada, from 2016 to 2017. He has been an Assistant Professor with the Department of Electrical and Computer Engineering, University of Nebraska-Lincoln, Lincoln, NE, USA, since 2017. His research interests include security and privacy for mobile social networks, e-healthcare systems, cloud/edge computing, and cyber physical systems.

Nan Cheng (S'12–M'16) received the B.E. and M.S. degrees from the Department of Electronics and Information Engineering, Tongji University, Shanghai, China, in 2009 and 2012, respectively, and the Ph.D. degree from the Department of Electrical and Computer Engineering, University of Waterloo, in 2015. He is currently a Post-Doctoral Fellow with the Department of Electrical and Computer Engineering, University of Toronto, and the Department of Electrical and Computer Engineering, University of Waterloo, under the supervision of Prof. B. Liang and Prof. S. Shen. His current research focuses on big data in vehicular networks and self-driving system. His research interests also include performance analysis, MAC, opportunistic communication, and application of AI for vehicular networks.

Xiaoming Yuan (S'17) received the B.E. degree in electronics and information engineering from Henan Polytechnic University, China, in 2012, and the Ph.D. degree in communication and information system from Xidian University, China, in 2018. From 2016 to 2017, she was a Visiting Scholar with the Broadband Communications Research Group, Department of Electrical and Computer Engineering, University of Waterloo, Waterloo, ON, Canada. Her research interests include cloud/edge computing, medium access control and performance analysis for wireless body area networks, and the Internet of Things.

Ning Zhang (M'15) received the Ph.D. degree from the University of Waterloo, Canada, in 2015. He was a Post-Doctoral Research Fellow with the University of Waterloo and the University of Toronto, Canada. He is currently an Assistant Professor with Texas A&M University–Corpus Christi, TX, USA. His current research interests include next generation mobile networks, physical layer security, machine learning, and mobile edge computing. He was a recipient of the Best Paper Awards at IEEE GLOBECOM 2014 and IEEE WCSP 2015. He served as the Workshop Chair for the first IEEE Workshop on Cooperative Edge and the IEEE Workshop on Mobile Edge Networks and Systems for Immersive Computing and IoT. He serves/served as an Associate Editor of the IEEE ACCESS, *IET Communication*, and the *Journal of Advanced Transportation*, an Area Editor of the *Encyclopedia of Wireless Networks* (Springer) and Cambridge Scholars, and a Guest Editor of *Wireless Communication and Mobile Computing*, the *International Journal of Distributed Sensor Networks*, and *Mobile Information System*.

Changle Li (M'09–SM'16) received the Ph.D. degree in communication and information system from Xidian University, China, in 2005. He conducted his postdoctoral research in Canada and the National Institute of information and Communications Technology, Japan, respectively. He had been a Visiting Scholar with the University of Technology Sydney. He is currently a Professor with the State Key Laboratory of Integrated Services Networks, Xidian University. His research interests include intelligent transportation systems, vehicular networks, mobile ad hoc networks, and wireless sensor networks.

Xuemin (Sherman) Shen (M'97–SM'02–F'09) received the B.Sc. degree in electrical engineering from Dalian Maritime University, China, in 1982, and the M.Sc. and Ph.D. degrees in electrical engineering from Rutgers University, NJ, USA, in 1987 and 1990, respectively. He is currently a University Professor and the Associate Chair for Graduate Studies, Department of Electrical and Computer Engineering, University of Waterloo, Canada. His research focuses on wireless resource management, wireless network security, social networks, smart grid, and vehicular ad hoc and sensor networks. He is a registered professional engineer of Ontario, Canada, an Engineering Institute of Canada Fellow, a Canadian Academy of Engineering Fellow, and a Royal Society of Canada Fellow. He received the IEEE ComSoc Education Award, the Joseph LoCicero Award for Exemplary Service to Publications, the Excellent Graduate Supervision Award in 2006, and the Premiers Research Excellence Award in 2003 from the Province of Ontario, Canada. He was the elected IEEE ComSoc Vice President of Publications and was a member of the IEEE ComSoc Board of Governors. He was the Chair of the Distinguished Lecturers Selection Committee. He is a Distinguished Lecturer of IEEE Vehicular Technology Society and Communications Society. He served as the Technical Program Committee Chair/Co-Chair for the IEEE Globecom16, Infocom14, the IEEE VTC10 Fall, and Globecom07, the Symposia Chair for the IEEE ICC10, the Tutorial Chair for the IEEE VTC11 Spring and the IEEE ICC08, the General Co-Chair for the ACM Mobihoc15, Chinacom07, and QShine06, and the Chair for the IEEE Communications Society Technical Committee on Wireless Communications and P2P Communications and Networking. He also serves/served as the Editor-in-Chief for the IEEE INTERNET OF THINGS JOURNAL, the *IEEE Network Magazine*, *Peer-to-Peer Networking and Application*, and *IET Communications*; a Founding Area Editor for the IEEE TRANSACTIONS ON WIRELESS COMMUNICATIONS; and an Associate Editor for the IEEE TRANSACTIONS ON VEHICULAR TECHNOLOGY and the IEEE WIRELESS COMMUNICATIONS.